

IN SILICO PROTEIN INTERACTION ANALYSIS OF DENGUE VIRUS NON-STRUCTURAL 2A AND HUMAN POTASSIUM CHANNEL KV1.3

Nur Al Syifaa Hassan^a, Suzana Misbah^{a*}, Siti Aisyah Razali^a, Boon-Teong Teoh^b, Sazaly AbuBakar^b

^aBiological Security and Sustainability (BioSES) Research Interest Group, Faculty of Science and Marine Environment, Universiti Malaysia Terengganu, 21030 Kuala Nerus, Terengganu, Malaysia

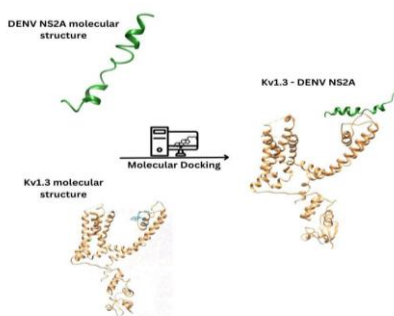
^bHigher Institution Centre of Excellence (HiCoE), Tropical Infectious Diseases Research & Education Centre (TIDREC), Universiti Malaya, 50603 Kuala Lumpur, Malaysia

Article history

Received
5 November 2023
Received in revised form
31 January 2024
Accepted
20 February 2024
Published Online
23 June 2024

*Corresponding author
suzana_m@umt.edu.my

Graphical abstract



Abstract

Dengue virus (DENV) is a mosquito-borne pathogen that causes dengue fever, a potentially severe illness. During infection, DENV interacts with various host factors to facilitate viral production. However, certain host restriction factors, such as the voltage-gated potassium channel Kv1.3, can impede viral replication by limiting DENV entry into host cells. While the interplay of DENV proteins and the specific mechanism facilitating this event remain unclear, our previous yeast two-hybrid interactomes study identified an interaction between DENV non-structural protein 2A (NS2A) and Kv1.3. This study aimed to identify potential binding sites between DENV NS2A and Kv1.3 using *in silico* approach. Crystal structures of DENV NS2A and Kv1.3 was obtained from RCSB PDB. Protein-protein interaction analysis was conducted using molecular docking with HADDOCK v2.4, and the interaction was assessed based on HADDOCK scores. Our results revealed that the HADDOCK score was -64.7 ± 3.2 , indicating an excellent binding affinity between DENV NS2A and Kv1.3. The robust interaction between NS2A and Kv1.3 underscores the need for further investigation into the role of potassium channels in DENV replication.

Keywords: Potassium channel, dengue virus, molecular docking, protein-protein interaction, human-virus interaction

Abstrak

Virus denggi (DENV) ialah patogen bawaan nyamuk yang mengakibatkan demam denggi, iaitu penyakit yang berpotensi menjadi semakin tenat. Semasa jangkitan, DENV berinteraksi dengan pelbagai faktor perumah untuk membantu penghasilan virus. Namun begitu, terdapat faktor sekatan perumah tertentu seperti saluran kalium voltan berpagar Kv1.3 yang boleh menghalang replikasi virus dan menahkalkan DENV daripada memasuki ke dalam sel perumah. Walaupun interaksi di antara protein-protein DENV dan mekanisma tertentu yang menyebabkan berlakunya perkara ini masih tidak jelas, hasil interaksi sebelum ini melalui dua-hibrid yis telah menunjukkan bahawa protein DENV tidak berstruktur 2A (NS2A) berinteraksi dengan Kv1.3. Kajian pada kali ini bertujuan untuk mengenal pasti tapak pengikatan yang berpotensi antara DENV NS2A dan Kv1.3 menggunakan pendekatan *in silico*. Struktur kristal DENV NS2A dan Kv1.3 telah diperolehi daripada RCSB PDB. Interaksi antara protein-protein tersebut telah dianalisa menggunakan dok molekul HADDOCK v2.4, dan interaksi tersebut dinilai

melalui skor HADDOCK. Hasil kajian kami menunjukkan bahawa skor HADDOCK ialah -64.7 ± 3.2 , yang menyatakan pertalian pengikatan yang sangat baik antara DENV NS2A dan Kv1.3. Interaksi yang teguh antara DENV NS2A dan Kv1.3 menunjukkan kepentingan untuk menjalankan kajian lanjut mengenai peranan saluran kalium dalam replikasi DENV.

Kata kunci: Saluran kalium, virus denggi, dok molekul, interaksi antara protein, interaksi antara manusia dan virus

© 2024 Penerbit UTM Press. All rights reserved

1.0 INTRODUCTION

Dengue is a mosquito-borne viral disease that represents a significant public health concern. The disease has broad spectrum of illnesses ranging from mild dengue fever to severe dengue haemorrhagic fever and dengue shock syndrome. Treatment of dengue is mainly supportive due the lack of specific antiviral therapy. Dengue is a disease caused by dengue virus (DENV) which spreads to humans through the bite of an infected *Aedes* mosquito. The virus belongs to the genus *Flavivirus* of the family *Flaviviridae* and is characterized by the presence of four distinct serotypes (DENV-1 to DENV-4). DENV genome consists of a single-stranded positive-sense RNA that contains a single open reading frame, encoding a polyprotein which is then cleaved to produce three structural proteins (capsid, pre-membrane, and envelope), and seven non-structural (NS) proteins (NS1, NS2A, NS2B, NS3, NS4A, NS4B, and NS5).

NS2A in particular, is a small transmembrane protein mainly localizes to the host endoplasmic reticulum (ER). The NS2A N-terminus is cleaved by host protease and localized on the ER lumen, while the C-terminus is cleaved by the viral NS2B-NS3 protease found in the cytoplasm [1]. Although knowledge about DENV NS2A is limited, the protein has shown to play important roles in the viral life cycle including RNA replication and assembly. NS2A interacts with other viral proteins, recruiting the genomic RNA, structural proteins, and NS2B-NS3 protease to the site of virus assembly which coordinates virus formation [2]. Increasing evidence has also documented the role of NS2A in immune evasion and modulation of the host immune response during DENV infection [3].

Most viruses can interact with host cellular factors causing changes in the expression levels, hence facilitating virus replication and dissemination. In particular, potassium (K^+) channels are one such host factors that play a significant role in virus infection [4]. K^+ channels represent a large group of transmembrane proteins responsible in transporting K^+ ions across the plasma membrane and subcellular compartments, hence controlling cellular ion homeostasis. Previous studies have shown that several negative-strand viruses including Bunyamwera virus,

Schmallenberg, and Hazara virus are dependent on the cellular two-pore K^+ (K_{2P}) channels during infection, highlighting their crucial role in early events after virus entry [5]. Exposure to high K^+ ion concentrations regulated by cellular K^+ channels causes virus accumulation through endosomes which influence the infectivity of virions [6].

While virus requirement for K^+ channels has been documented, other studies have shown that some channels including the voltage-gated K^+ channel serves a host restriction factor that limits viral production [7, 8]. This channel acts by inhibiting the endosome acidification following viral entry, thus prevents viral fusion/uncoating process and restricts viral replication [8]. Certain viral proteins however are capable of counteracting K^+ channel activity such as NS5A of Hepatitis C virus (HCV) that inhibits phosphorylation of a different potassium channel Kv2.1, resulting in suppression of apoptosis [9]. It is evident that HCV NS5A interacts with the host protein mixed lineage kinase 3, leading to the suppression of p38MAPK signalling and disruption of Kv2.1-induced apoptosis, which ultimately promotes the virus survival [10].

Whilst experiments investigating virus-host protein-protein interactions are crucial for comprehending viral pathogenesis within the cellular host, data from these interactions can be supported by *in silico* computational tools. These analyses are important to understand certain mechanism of viral infection by targeting the specific protein interactions between viruses and host cells. Our previous study has shown that DENV NS2A interacts with the human voltage-gated K^+ channel Kv1.3 using the high-throughput yeast two-hybrid screen [11]. In the present study, we aimed to analyse NS2A-Kv1.3 protein-protein interaction via *in silico* approach. Data from this study could provide insights into the prediction of NS2A-Kv1.3 interaction in DENV-infected host.

2.0 METHODOLOGY

Protein Structures

Three-dimensional (3D) structures of DENV NS2A protein and the voltage-gated K^+ channel Kv1.3 were

obtained from the Research Collaboratory Structural Bioinformatics-Protein Data Bank (RCSB PDB). The solution structure of DENV NS2A transmembrane domain (PDB ID: 2M0S) was obtained from: <https://www.rcsb.org/structure/2m0s> as previously established by Xie *et al.*, 2013 [1]. Whereas, the human voltage-gated K⁺ channel Kv1.3 (PDB ID: 7EJ1) has been recently generated which was obtained here: <https://www.rcsb.org/structure/7EJ1> [12]. Both NS2A and Kv1.3 protein sequences were downloaded in FASTA format and the structure models were generated in Chimera ver1.16. The 7EJ1 was assembled as a tetramer with four-fold symmetry, and among two unique structures which are 7EJ1_1 (chains A, C, E, G) and 7EJ1_2 (chains B, D, F, H). The chain B from 7EJ1_2 was appointed as a monomer for the Kv1.3 structure because it exhibits similar properties to the native Kv1.3 channel in human T lymphocytes and shares high sequence identity with a crystal structure of the human Kv1.2/2.1 chimera channel [13]. Chain B was chosen from the 7EJ1_2 structure, which corresponds to the B subunit of the channel, as similar to Kv1.3 because it shares high sequence identity with Kv1.3 and is located in a similar position in the channel as Kv1.3. Water molecules were removed from both structures using UCSF Chimera (<https://www.rbvi.ucsf.edu/chimera>) to reduce the complexities in the binding studies. The PDB file has been prepared for HADDOCK, as the HADDOCK webserver requires this file as an input. HADDOCK was employed in our study due to its established success in modelling diverse biomolecular complexes, as articulated by Kurkcuoglu *et al.* (2018) [14]. HADDOCK has demonstrated significant efficacy in predicting the structure of protein-protein, protein-nucleic acid, and protein-peptide complexes, as highlighted in numerous successful applications [15]. Notably, HADDOCK consistently ranks among the top scorers and predictors in the Critical Assessment of Predicted Interactions (CAPRI) experiments, thereby confirming its dependability and performance [16]. This strategy predicted multiple high-quality models for various targets in recent CAPRI experiments [17].

Molecular Docking

Molecular interaction analysis between DENV NS2A and Kv1.3 proteins was carried out using HADDOCK 2.4 (High Ambiguity Driven protein-protein DOCKing) webserver, freely accessible at <http://haddock.science.uu.nl/services/HADDOCK2.4>. The following active sites residues were selected for active ambiguous interaction restraints as input to HADDOCK: LYS16, ARG18 and PRO19 residues for NS2A, while TRP436, THR441, TYR447, GLY448, ASP449 and HIS451 residues for Kv1.3, as established previously by Xie *et al.*, (2013) for NS2A and Liu *et al.*, (2021) for Kv1.3 [1, 12]. HADDOCK clustered all docking simulations and ranked them based on HADDOCK score, which is a function of a linear combination of Van der Waals energy, electrostatic energy, desolvation energy, restraint violation energy, and

buried surface area (BSA). The cluster with the lowest HADDOCK score was chosen for further assessment [18, 19]. The models and complexes were visualized using UCSF Chimera. Next, the intermolecular contacts such as hydrogen bonds and those that are not bonded were determined using the LIGPLOT-DIMPLOT v4.5.3 programme for automatically plotting protein-protein interactions.

3.0 RESULTS AND DISCUSSION

Dengue Virus NS2A and Kv1.3 Structures

Physical interactions between DENV NS2A and the human K⁺ channel, Kv1.3 was investigated in this study. The structure of partial DENV NS2A was obtained from PDB ID: 2M0S through Chimera bioinformatic tool. As shown in Figure 1, the partial NS2A crystal structure (PDB ID: 2M0S) consists of 28 amino acid residues with the total structure weight 2.98 kDa, and 42% of these amino acids were hydrophobic. Blue regions indicate predicted key residues of 2M0S which were LYS16, ARG18 and PRO19, corresponded to the established K82, R84 and P85, respectively [1]. The structure was composed of two helices, with a helix breaker facilitated by residue PRO19, which separates the helices. Within this transmembrane region, two charged residues, LYS16 and ARG18 were positioned upstream of the breaker.

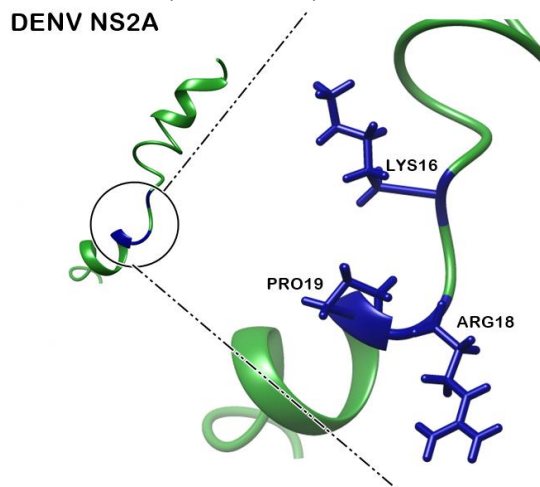


Figure 1 DENV NS2A crystal structure (PDB ID: 2M0S). Magnified view of the circled structure shows the predicted LYS16, ARG18 and PRO19 residues (in blue) corresponded to the active binding sites. The remaining regions are shown in green

NS2A integral protein (approximately 22 kDa) is hydrophobic, known to be closely associated with the ER membrane. While there is no complete NS2A crystal structure available, the established membrane topology of NS2A has provided useful information on the biological function. Based on the model, DENV NS2A generates five transmembrane segments in the ER membrane, where the N-terminal 68 residues are

located in the ER lumen, with one segment (residues 30-52) closely associates with the membrane [1]. Two transmembrane segments (residues 69-119), a non-transmembrane segment (residues 120-142), three transmembrane segments (residues 143-209) span the remaining regions, and the C-terminal tail (residues 210-218) ends in the cytosol. Within NS2A, the positively charged amino acid residue R84 has shown to play a critical role in both viral RNA synthesis and assembly [1]. The residue ARG18 identified in this study corresponds to the residue R84, as previously described [1]. Mutations introduced to NS2A has significantly impacted these processes, thus abolished production of infectious virions [20]. While NS2A is relatively small, the protein has been suggested to exhibit viroporin-like characteristics with membrane-stabilizing potential [21]. According to Meng *et al.* (2015), NS2A is highly structural as it has few disorder-promoting regions and those regions are rich in disorder-promoting residues [22]. The fact that disordered regions of the DENV proteins contain numerous phosphorylation sites agrees with observations that phosphorylation and many other enzymatically catalyzed post-translational modifications are preferentially located within IDPRs (intrinsically disordered protein regions). The predominant function of the DENV IDPRs is protein-protein binding and viral IDPRs are associated with phosphorylation [22].

On the other hand, Kv1.3 is a large membrane protein where its crystal structure has been recently established [12]. The total structure weight of Kv1.3 channel (PDB ID: 7EJ1) was 422.80 kDa with two unique protein chain molecules 7EJ1_1; voltage-gated potassium channel subunit beta-2 (chains A, C, E, G), and 7EJ1_2 potassium voltage-gated channel subfamily A member 3 (chains B, D, F, H). Both 7EJ1_1 and 7EJ1_2 represent 367 and 575 amino acid sequence, respectively. Based on Figure 2(a), 7EJ1_2 has a high accuracy resolution structure which is 3.3 Å. This value falls within the range 2.5 – 3.5 Å, which allows for accurate model building as previously described in [12]. As shown in Figure 2(b), Chain B was chosen as it represents the Kv1.3 tetramer structure that assembles four identical individual subunits as established [25]. The predictive active sites within the Kv1.3 protein structure 7EJ1 were identified as TRP436, THR441, TYR447, GLY448, ASP449 and HIS451 amino acid residues, as shown in Figure 2(c).

Kv1.3 is primarily expressed in T lymphocytes, and its role is intricately linked to the regulation of immune cell function [23]. The channel is also expressed in other cell types including fibroblasts, macrophages, microglia, megakaryocytes, and is responsible for the major K⁺ conductance and the resting potential in platelets [24]. Kv1.3 localizes to the plasma membrane and the membrane of subcellular organelles including endosomes, Golgi, nucleus and mitochondria. Kv1.3 are tetramers where each subunit has a large cytoplasmic domain T1 and six transmembrane helices [25]. Typically, Kv1.3 channel activates in response to membrane depolarization, permitting the

passage of K⁺ ions. The ion conductivity is reduced as they transition into non-conductive, inactivated states in a time-dependent manner.

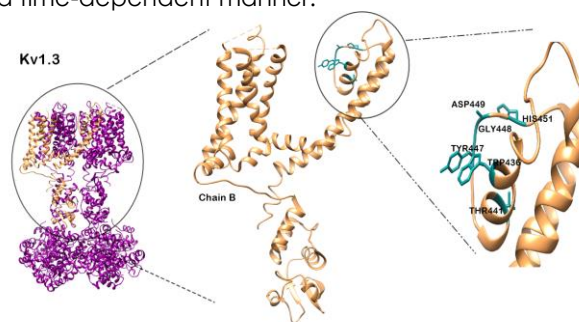


Figure 2 Kv1.3 crystal structure PDB ID: 7EJ1. (a) Kv1.3, (b) Magnified view of the circled structure represents Chain B of Kv1.3 tetramer, (c) An enlarged view of the circled structure exhibiting TRP436, THR441, TYR447, GLY448, ASP449 and HIS451 residues (in cyan) of the expected active sites

DENV NS2A-Kv1.3 Protein Interaction

Based on the crystal structure models in Figure 1 and Figure 2(a-c), the specific targeted binding sites of each protein were determined. The key residues of NS2A were identified as LYS16, ARG18 and PRO19, whereas for Kv1.3 structure include TRP436, THR441, TYR447, GLY448, ASP449 and HIS451. This information was sent to an information-driven flexible docking approach, HADDOCK for the modelling of biomolecular complexes. After a successful docking, HADDOCK clustered 81 structures into 8 clusters, which represents 40% of the water-refined models. The NS2A-Kv1.3 protein interaction complex shows the lowest HADDOCK score of -64.7 ± 3.2 , representing the good affinity level between the proteins. The BSA of Cluster 4 of the NS2A-Kv1.3 complex was 926.8 ± 60.7 , which indicates close proximity and a less water-exposed protein surface. The desolvation energy (-16.2 ± 4.1), restraint violation energy (20.9 ± 10.5), and BSA have a high-quality association with the docking score of the complex. The HADDOCK score, interaction energy, Van der Waals energy, electrostatic energy, desolvation energy, restraints violation energy, and BSA of the top 8 clusters are shown in Table 1. The HADDOCK best structure is shown in Figure 3.

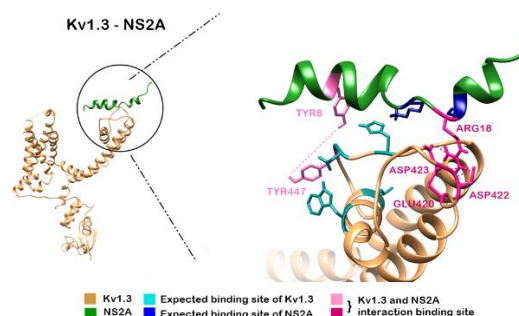


Figure 3 Protein-protein interaction between DENV NS2A and Kv1.3 based on HADDOCK, where the specific interaction region is circled. Enlarged view of this region is shown, exhibiting the NS2A-Kv1.3 binding sites (in light pink and dark pink)

Table 1 DENV NS2A-Kv1.3 protein-protein interaction model based on eight structures, which are arranged according to the best cluster determined by HADDOCK scores

Parameters	Cluster 4	Cluster 2	Cluster 3	Cluster 1	Cluster 6	Cluster 8	Cluster 7	Cluster 5
HADDOCK score	-64.7 ± 3.2	-64.6 ± 2.5	-62.7 ± 3.8	-60.6 ± 1.3	-55.4 ± 3.4	-47.7 ± 9.1	-47.6 ± 6.5	-35.7 ± 2.9
Cluster size	8	11	8	34	6	4	4	6
RMSD value	5.1 ± 0.3	7.3 ± 0.1	6.5 ± 0.4	4.5 ± 0.3	5.5 ± 0.2	6.0 ± 0.5	5.8 ± 0.2	5.0 ± 0.2
Van der Waals energy	-19.3 ± 2.3	-25.7 ± 0.6	-24.6 ± 5.7	-20.8 ± 0.9	-13.3 ± 2.5	-13.4 ± 1.4	-14.3 ± 1.8	-12.8 ± 2.8
Electrostatic energy	-156.2 ± 23.1	-173.5 ± 12.3	-159.3 ± 25.0	-161.5 ± 12.6	-201.9 ± 13.6	-120.5 ± 43.5	-124.8 ± 33.8	-91.9 ± 10.7
Desolvation energy	-16.2 ± 4.1	-5.4 ± 1.2	-6.5 ± 7.6	-8.4 ± 1.5	-2.8 ± 4.6	-12.3 ± 3.4	-8.7 ± 3.6	-4.7 ± 2.0
Restraints violation energy	20.9 ± 10.5	11.9 ± 14.6	2.4 ± 0.9	9.7 ± 11.6	11.3 ± 13.7	20.3 ± 30.5	3.4 ± 0.9	1.9 ± 0.3
Buried surface area	926.8 ± 60.7	1020.8 ± 103.4	1011.0 ± 159.0	779.9 ± 24.7	822.5 ± 40.0	705.7 ± 70.9	717.1 ± 42.6	530.0 ± 39.0
Z score	-1.0	-1.0	-0.8	-0.6	-0.1	0.7	0.7	2.0

From the HADDOCK results, the best molecular docking structure suggested between NS2A and Kv1.3 were residues TYR8 and TYR447. Meanwhile, another interaction occurs between residues ARG18 with GLU420, ASP422, and ASP423. The intermolecular contact between these structures is shown in Figure 4.

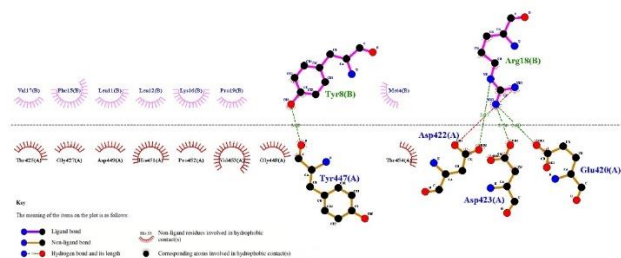


Figure 4 LIGPLOT prepared the best structures of the NS2A-Kv1.3 cluster interacting residues in the NS2A-Kv1.3 complex. The colour-coding represents NS2A in pink and Kv1.3 in brown. The dashed green line denotes hydrogen-bonding interaction

From the NS2A-Kv1.3 protein-protein interaction model, Cluster 4 was considered as the best model among the eight clusters with electrostatic energy exhibited -156.2 ± 23.1 . Lower electrostatic energy indicates a more favourable electrostatic force interaction and being a part of the total binding energy that has several different components [26].

The RMSD values for cluster 4 was 5.1 ± 0.3 (Table 1). Since RMSD values have no predictive values, it only indicates where a cluster is, with respect to the best model generated by HADDOCK. The HADDOCK score leads the way to determine the best cluster

model. As supported by Hussain *et al.*, (2020) and Rostaminia *et al.*, (2021), the cluster that has the lowest HADDOCK score was chosen [18, 19]. HADDOCK scoring function makes up by a linear combination of various energy and BSA. It differs in various docking stages, including explicit solvent refinement (water), rigid body (it0), and semi-flexible refinement (it1). From established information, the scoring is calculated based on the weighted sum (<https://www.bonvinlab.org/software/haddock2.4/scoring/>).

There is residues interaction between two-docked protein structures of NS2A-Kv1.3 as shown in Table 2.

Table 2 Hydrogen bond interaction values between residues of NS2A and Kv1.3

NS2A residue	Kv1.3 residue	Hydrogen bond interaction values (Ångströms)
ARG18	GLU420	2.60
ARG18	ASP422	3.07
ARG18	ASP423	2.74
TYR8	TYR447	3.02

The positively charged residue ARG18 from NS2A protein interacts with GLU420, ASP422, and ASP423 residues of Kv1.3 protein which are negatively charged. This interaction forms due to the presence of opposite charged residues making them electrostatically attracted. Another strong interaction

occurs between residues TYR8 of NS2A and TYR447 of Kv1.3 protein. Both TYR8 and TYR447 are hydrophobic residues that make significant contribution to the formation of hydrogen bond. The amino acid tyrosine is considered as hydrophobic based on their hydrophathy features as well as aromatic interactions. Interactions between these amino acid residues have a significant influence on the protein interaction complex, which contribute significantly to the conformational stability of the protein structure [27]. The Kv1.3 channel shows several potential tyrosine phosphorylation domains and tyrosine phosphorylation exerts diverse effect on ion channels, encompassing rapid current fluctuations to protracted alteration in targeting and protein synthesis. This post-translational modification often triggers metabolic reprogramming in cancer cells and also indirectly involved in mitogen-activated protein kinases (MAPK) cascade of cell apoptosis and proliferation. Concurrently, co-expression of Kv1.3 with viral sarcoma resulting increases of channel phosphorylation due to the tyrosine kinases and remarks that the heightened phosphorylation causes Kv1.3 current suppression [28]. While the hydrophobic effect is the most important driving force in protein folding, electrostatic interactions are equally important in protein folding, stability, flexibility, and function. The hydrophobicity of the binding regions dictates shape complementary as much as the correlation between van der Waals energy and binding affinity [29]. Based on our analyses, NS2A and Kv1.3 exhibit a significant binding affinity, indicating a strong interaction between the viral and host proteins.

Virus-host protein-protein interactions are crucial events in the life cycle of many viruses, impacting various aspects of infection, replication, and pathogenesis. These interactions allow viruses to recruit host factors and manipulate host cell signalling pathways. Given the ability of DENV in modulating Ca^{2+} ion homeostasis that facilitates viral replication [30], it is known that maintaining a cellular environment suitable for virus persistence partially relies on the virus ability to manipulate the ion channel activity. While the role of the voltage-gated Kv1.3 K^+ channel in viral infection is limited, previous study has demonstrated that the over-expression of this channel has resulted in the alkalization of acidic organelles by gaining luminal cations, which subsequently prevent endosome acidification [8]. This condition prevents fusion of the membrane of viral envelope and the host endosomal membrane which has resulted in restriction of HCV virus production following the viral entry. It is important to note that the same effect was not observed with Sendai virus which suggests that the inhibition is virus-specific. Nonetheless, similar findings were obtained in the cases of DENV and Zika virus, indicating they exhibit outcomes similar to HCV [8].

In this study, we have established the interaction between DENV NS2A and Kv1.3 *in silico*. However, this observation requires confirmation through laboratory experiments, such as co-immunoprecipitation assays. Further analysis of the virus replication in abrogated

Kv1.3 will demonstrate functional importance of this channel in restricting DENV infection. Overall, dissecting the role of viral proteins and their physical interaction with host protein targets is essential to uncover key factors involved in virus infection. This knowledge can lead to the identification of potential drug targets for antiviral therapies and the development of strategies to disrupt essential protein-protein interactions, thereby limiting viral infections.

4.0 CONCLUSION

Structural binding between DENV NS2A and human Kv1.3 has been demonstrated in this study using *in silico* approach. The findings were validated through molecular docking, resulting a significant HADDOCK score. These results encourage future research to better understand the role of K^+ channels in DENV replication.

Conflicts of Interest

The author(s) declare(s) that there is no conflict of interest regarding the publication of this paper.

Acknowledgements

We would like to thank the Ministry of Higher Education, Malaysia under the Fundamental Research Grant Scheme, FRGS/1/2018/STG03/UMT/03/3 for funding this research. This work was also supported by the Ministry of Higher Education, Malaysia for niche area research under the Higher Institution Centre of Excellence (HICoE) program (MO002–2019 & TIDREC-2023). We thank the Faculty of Science and Marine Environment, Universiti Malaysia Terengganu for providing the research facilities.

References

- [1] Xie, X., S. Gayen, C. Kang, Z. Yuan, and P.-Y. Shi. 2013. Membrane Topology and Function of Dengue Virus NS2A Protein. *Journal of Virology*. 87: 4609-4622. <https://doi.org/10.1128/JVI.02424-12>.
- [2] Xie, X., J. Zou, X. Zhang, Y. Zhou, A. L. Routh, C. Kang, V. L. Popov, X. Chen, Q.-Y. Wang, H. Dong, and P.-Y. Shi. 2019. Dengue NS2A Protein Orchestrates Virus Assembly. *Cell Host & Microbe*. 26: 606-622.e8. <https://doi.org/10.1016/j.chom.2019.09.015>.
- [3] Lee, M. F., G. Z. Voon, H. X. Lim, M. L. Chua, and C. L. Poh. 2022. Innate and Adaptive Immune Evasion by Dengue Virus. *Frontiers in Cellular and Infection Microbiology*. 12. <https://doi.org/10.3389/fcimb.2022.1004608>.
- [4] Charlton, F. W., H. M. Pearson, S. Hover, J. D. Lippiat, J. Fontana, J. N. Barr, and J. Mankouri. 2020. Ion Channels as Therapeutic Targets for Viral Infections: Further Discoveries and Future Perspectives. *Viruses*. 12: 844. <https://doi.org/10.3390/v12080844>.

- [5] Hover, S., B. King, B. Hall, E. Loundras, H. Taqi, J. Daly, M. Dallas, C. Peers, E. Schnettler, C. Mckimmie, A. Kohl, J. N. Barr, and J. Mankouri. 2016. Modulation of Potassium Channels Inhibits Bunyavirus. *Journal of Biological Chemistry*. 291: 3411-3422. <https://doi.org/10.1074/jbc.M115.692673>.
- [6] Hover, S., B. Foster, J. Fontana, A. Kohl, S. A. N. Goldstein, J. N. Barr, and J. Mankouri. 2018. Bunyavirus Requirement for Endosomal K⁺ Reveals New Roles of Cellular Ion Channels during Infection. *PLOS Pathogens*. 14: e1006845. <https://doi.org/10.1371/journal.ppat.1006845>.
- [7] Hover, S., B. Foster, J. N. Barr, and J. Mankouri. 2019. Viral Dependence on Cellular Ion Channels - An Emerging Anti-Viral Target? *Journal of General Virology*. 345-351. <https://doi.org/10.1099/jgv.0.000712>.
- [8] Lang, Y., F. Li, Q. Liu, Z. Xia, Z. Ji, J. Hu, Y. Cheng, M. Gao, F. Sun, B. Shen, C. Xie, W. Yi, Y. Wu, J. Yao, and Z. Cao. 2020. The Kv1.3 Ion Channel Acts as a Host Factor Restricting Viral Entry. *The FASEB Journal*. 1-17. <https://doi.org/10.1096/fj.202000879RR>.
- [9] Mankouri, J., M. L. Dallas, M. E. Hughes, S. D. C. Griffin, A. Macdonald, C. Peers, and M. Harris. 2009. Suppression of a Pro-apoptotic K⁺ Channel as a Mechanism for Hepatitis C Virus Persistence. *Proceedings of the National Academy of Sciences USA*. 106: 15903-15908. <https://doi.org/10.1073/pnas.0906798106>.
- [10] Amako, Y., Z. Igloi, J. Mankouri, A. Kazlauskas, K. Saksela, M. Dallas, C. Peers, and M. Harris. 2013. Hepatitis C Virus NS5A Inhibits Mixed Lineage Kinase 3 to Block Apoptosis. *Journal of Biological Chemistry*. 288: 24753-24763. <https://doi.org/10.1074/jbc.M113.491985>.
- [11] Misbah, S. 2015. Host Cellular Regulatory Networks in Dengue Virus-human Interactions. Doctoral dissertation. University of Glasgow. <http://theses.gla.ac.uk/id/eprint/7330>.
- [12] Liu, S., Y. Zhao, H. Dong, L. Xiao, Y. Zhang, Y. Yang, S. T. Ong, K. G. Chandy, L. Zhang, and C. Tian. 2021. Structures of Wild-type and H451N Mutant Human Lymphocyte Potassium Channel KV1.3. *Cell Discovery*. 7: 0-4. <https://doi.org/10.1038/s41421-021-00269-y>.
- [13] Matthies, D., C. Bae, G. E. Toombes, T. Fox, A. Bartesaghi, S. Subramaniam, and K. J. Swartz. 2018. Single-particle Cryo-EM Structure of a Voltage-activated Potassium Channel in Lipid Nanodiscs. *eLife*. 7: e37558. <https://doi.org/10.7554/eLife.37558>.
- [14] Kurkcuoglu, Z., Koukos, P. I., Citro, N., Trellet, M., Rodrigues, J. P. G. L. M., Moreira, I. S., Roel-Touris, J., Melquiond, A., Geng, C., Schaarschmidt, J., Li, X., Vangone, A., & Bonvin, A. M. J. 2017. Performance of HADDOCK and a Simple Contact-based Protein-ligand Binding Affinity Predictor in the D3R Grand Challenge 2. *Journal of Computer-Aided Molecular Design*. 32(1): 175-185. <https://doi.org/10.1007/s10822-017-0049-y>.
- [15] Moreira, I. S., Fernandes, P. A., & Ramos, M. J. 2009. Protein-protein Docking Dealing with the Unknown. *Journal of Computational Chemistry*. 31(2): 317-342. <https://doi.org/10.1002/jcc.21276>.
- [16] Vangone, A., Rodrigues, J. P. G. L. M., Li, X., Van Zundert, G. C. P., Geng, C., Kurkcuoglu, Z., Nellen, M., Narasimhan, S., Karaca, E., Van Dijk, M., Melquiond, A., Visscher, K., Trellet, M., Kastriitis, P. L., & Bonvin, A. 2016. Sense and Simplicity in HADDOCK Scoring: Lessons from CASP-CAPRI Round 1. *Proteins: Structure, Function, and Bioinformatics*. 85(3): 417-423. <https://doi.org/10.1002/prot.25198>.
- [17] Lensink, M. F., Nadzirin, N., Velankar, S., & Wodak, S. J. 2020. Modeling Protein-protein, Protein-peptide, and Protein-oligosaccharide Complexes: CAPRI 7th Edition. *Proteins: Structure, Function, and Bioinformatics*. 88(8): 916-938. <https://doi.org/10.1002/prot.25870>.
- [18] Hussain, M., Jabeen, N., Amanullah, A., Baig, A. A., Aziz, B., Shabbir, S., Raza, F., & Uddin, N. 2020. Molecular Docking between Human TMPRSS2 and SARS-CoV-2 Spike Protein: Conformation and Intermolecular Interactions. *AIMS Microbiology*. 6(3): 350-360. <https://doi.org/10.3934/microbiol.2020021>.
- [19] Rostaminia, S., Aghaei, S. S., Farahmand, B., Nazari, R., & Ghaemi, A. 2021. Computational Design and Analysis of a Multi-epitope Against Influenza A virus. *International Journal of Peptide Research and Therapeutics*. 27(4): 2625-2638. <https://doi.org/10.1007/s10989-021-10278-w>.
- [20] Wu, R., M. Tsai, K.-N. Tsai, J. Tian, J.-S. Wu, S.-Y. Wu, J. H. Chen, C.-H. Chen, and A. Yueh. 2017. Mutagenesis of Dengue Virus Protein NS2A Revealed a Novel Domain Responsible for Virus-Induced Cytopathic Effect and Interactions between NS2A and NS2B Transmembrane Segments. *Journal of Virology*. 91: 1-24. <https://doi.org/10.1128/JVI.01836-16>.
- [21] Shrivastava G., J. García-Cordero, M. León-Juárez, G. Oza, J. Tapia-Ramírez, N. Villegas-Sepulveda, L. Cedillo-Barrón. 2017. NS2A Comprises a Putative Viroporin of Dengue Virus 2. *Virulence*. 8: 1450-1456. <https://doi.org/10.1080/21505594.2017.1356540>.
- [22] Meng, F., Badierah, R. A., Almehdar, H. A., Redwan, E. M., Kurgan, L., & Uversky, V. N. 2015. Unstructural Biology of the Dengue Virus Proteins. *The FEBS Journal*. 282(17): 3368-3394. <https://doi.org/10.1111/febs.13349>.
- [23] Gubič, Š., L. A. Hendrickx, Ž. Toplak, M. Sterle, S. Peigneur, T. Tomašič, L. A. Pardo, J. Tytgat, A. Zega, and L. P. Mašič. 2021. Discovery of Kv1.3 Ion Channel Inhibitors: Medicinal Chemistry Approaches and Challenges. *Medicinal Research Reviews*. 41: 2423-2473. <https://doi.org/10.1002/med.21800>.
- [24] McCloskey, C., S. Jones, S. Amisten, R. T. Snowden, L. K. Kaczmarek, D. Erlinge, A. H. Goodall, I. D. Forsythe, and M. P. Mahaut-Smith. 2010. Kv1.3 is the exclusive voltage-gated K⁺ channel of platelets and megakaryocytes: roles in membrane potential, Ca²⁺ signalling and platelet count. *The Journal of Physiology*. 588: 1399-1406. <https://doi.org/10.1113/jphysiol.2010.188136>.
- [25] Selvakumar, P., A. I. Fernández-Mariño, N. Khanra, C. He, A. J. Paquette, B. Wang, R. Huang, V. V. Smider, W. J. Rice, K. J. Swartz, and J. R. Meyerson. 2022. Structures of the T Cell Potassium Channel Kv1.3 with Immunoglobulin Modulators. *Nature Communications*. 13: 3854. <https://doi.org/10.1038/s41467-022-31285-5>.
- [26] Chakavorty, A., Li, L., & Alexov, E. 2016. Electrostatic Component of Binding Energy: Interpreting Predictions from Poisson-boltzmann Equation and Modeling Protocols. *Journal of Computational Chemistry*. 37(28): 2495-2507. <https://doi.org/10.1002/jcc.24475>.
- [27] Anjana, R., M. K. Vaishnavi, D. Sherlin, S. P. Kumar, K. Naveen, P. S. Kanth, and K. Sekar. 2012. Aromatic-aromatic Interactions in Structures of Proteins and Protein-DNA Complexes: A Study based on Orientation and Distance. *Bioinformation*. 8: 1220-1224. <https://doi.org/10.6026/97320630081220>.
- [28] Navarro-Pérez, M., Estadella, I., Benavente-Garcia, A., Orellana, R., Petit, A., Ferreres, J. C., & Felipe, A. 2023. The Phosphorylation of KV1.3: A Modulatory Mechanism for a Multifunctional Ion Channel. *Cancers*. 15(10): 2716. <https://doi.org/10.3390/cancers15102716>.
- [29] Desantis, F., Miotto, M., Di Rienzo, L., Milanetti, E., & Ruocco, G. 2022. Spatial Organization of Hydrophobic and Charged Residues Affects Protein Thermal Stability and Binding Affinity. *Scientific Reports*. 12(1). <https://doi.org/10.1038/s41598-022-16338-5>.
- [30] Dionicio, C. L., F. Peña, L. A. Constantino-Jonapa, C. Vazquez, M. Yocupicio-Monroy, R. Rosales, J. L. Zambrano, M. C. Ruiz, R. M. del Angel, and J. E. Ludert. 2018. Dengue Virus Induced Changes in Ca²⁺ Homeostasis in Human Hepatic Cells that Favor the Viral Replicative Cycle. *Virus Research*. 245: 17-28. <https://doi.org/10.1016/j.virusres.2017.11.029>.

